Orbital
The electronic journal of chemistry

the electronic journal of chemistry

Full Paper | http://dx.doi.org/10.17807/orbital.v13i3.1614

Synthesis, Antimicrobial, and DFT Studies of Some Benzyl 4-*O*-Acyl-α-L-rhamnopyranosides

Deen Muhammad, Mohammed M. Matin*, Sheikh Md. Rasel Miah, and Puja Devi

Application of carbohydrate fatty acid (CFA) esters in food and beverage industries has increased their interest in other fields. Especially rhamnopyranoside esters having both the hydrophilic and lipophilic nature had broader applications including anticancer activities. Benzyl α-L-rhamnopyranoside, prepared from L-rhamnose, on 2,3-*O*-isopropylidene protection with 2,2-dimethoxypropane followed by acylation at C-4 hydroxyl position with different acylating agents furnished the corresponding 4-*O*-acyl-α-L-rhamnopyranosides in good yields. All the compounds were well characterized by spectroscopic techniques. *In vitro* antimicrobial activities against eight bacterial and two fungal pathogens indicated that these 2,3-*O*-isopropylidene protected rhamnopyranosides had weak to moderate inhibitory properties. To rationalize such moderate activities structural (conformational) distortion of these monoacetonide protected CFA esters were studied from the density functional theory (DFT) optimized structures. In addition, thermodynamic properties including frontier molecular orbitals of the synthesized rhamnopyranosides were calculated and discussed. Corroboration of all the studies signifies that the moderate antimicrobial efficacy of the isopropylidene protected rhamnopyranosides might be due to their distorted conformations, lower softness and smaller dipole moments.

Graphical abstract

Keywords

Acylation
Antimicrobial agent
Benzyl α-L-rhamnopyranoside
Conformational study
HOMO-LUMO
Thermodynamic calculations

Article history

Received 04 April 2021
Revised 06 June 2021
Accepted 07 June 2021
Available online 25 June 2021

Handling Editor: Cauê A. Martins

1. Introduction

Natural and synthetic carbohydrate fatty acid (CFA) esters have become a research focus owing to their structural diversity, together with distinctive and remarkable pharmacodynamics actions, such as anti-depression, anticancer, antioxidant, anti-inflammatory and antiviral activities [1-4]. They have one or more acyl group(s) (aglycone moiety) attached to the carbohydrate skeleton via hydroxyl groups [5]. Due to the presence of both the hydrophilic and lipophilic moieties many CFA esters are used in detergent and cosmetic products, food and beverage industries, and

Bioorganic and Medicinal Chemistry Laboratory, Department of Chemistry, Faculty of Science, University of Chittagong, Chittagong, 4331, Bangladesh. *Corresponding author. E-mail: **mahbubchem@cu.ac.bd** ; Tel. +880 1716 839689

pharmaceutical industries [6-8]. The use of the CFA esters are comparatively inexpensive and thus, is an attractive strategy to reduce the production costs associated with biosurfactant and other products production. Their pharmaceutical applications mainly depend on their suitable antimicrobial and insecticidal activities [9]. CFA esters have also attracted considerable interest due to their non-toxic, biodegradable, non-allergic, and non-irritating nature [10-11]. It was observed that sugar ester part(s) of uridine (**1**, Figure 1) is more potent against SARS-CoV-2 main protease (Mpro; 7BQY) [12]. Therefore, the CFA esters have always been important component(s) of drugs [13], and their design, and synthesis play an important role in the diagnosis, prevention and treatment of diseases [14-16].

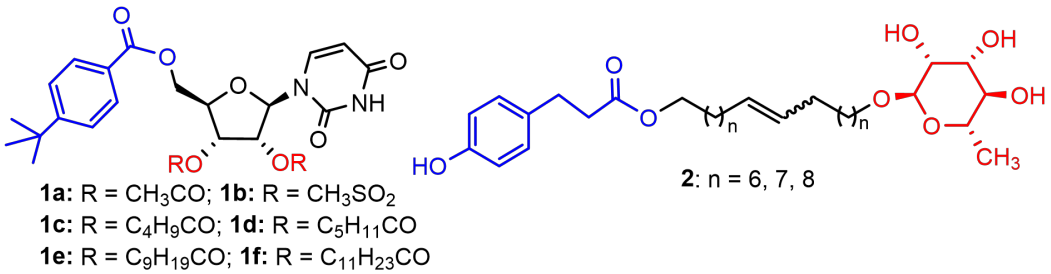

Fig. 1. Structure of CFA esters **1a-f**, and **2**.

Of the CFA esters rhamnopyranoside (6-deoxy sugar) related esters are particularly important and many researchers reported their neuroprotective [17], antidepressant [18-19], anticarcinogenic [20], antimicrobial [21], and pharmacological properties [22] as well as in bioremediation of pollutants. For example, rhamnopyranose 4-*O*-, 2,3-di-*O*- and 2,3,4-tri-*O*-acyl esters isolated from roots of *Scrophularia buergeriana* were found to reduce glutamate-induced neurotoxicity [17]. Thus, various plants extracts with rhamnose esters have been used in Oriental medicine as a treatment for fever, swelling, constipation, pharyngitis, neuritis and laryngitis [23-24]. In addition, recently, the synthesis and interfacial properties of rhamnopyranoside derived bolaamphiphile type biosurfactant materials (e.g. **2**, Figure 1) are reported [25]. However, no precise correlation has been made between a particular constituent of these compounds and an observed pharmacological activity except for effects on immunological activity, and hence further study is essential [26].

Various methods are reported, so far, for the selective and regioselective acylation of rhamnopyranosides and other monosaccharides [27] although the presence of several 2° hydroxyl groups of almost similar reactivity affecting functionalization (esterification) step leading to a mono-, di-, and polyesters [27]. Among them (i) catalyst mediated method [28-29], (ii) enzymatic method [30], (iii) microwave assisted method [31], (iv) direct method [32-33], and protection-deprotection method [34-35] are mainly used. It was reported that dibutyltin oxide method generally gave regioselectivity at C-3 hydroxyl position of rhamnopyranosides [29]. Hence, protection-deprotection is generally used for C-4 hydroxyl acylation [35].

Rhamnose occurs in nature in its L-form (6-deoxy-L-mannose) which seems to be unusual as most of the naturally occurring sugars exist in D-form. It exists in two anomeric forms, α-L-rhamnose and β-L-rhamnose. Generally, it bounds to other sugars and is a common glycone component of glycosides from many plants. Also, it is an important component of the outer cell membrane of acid-fast bacteria in the Mycobacterium genus [36]. Rhamnose containing chemicals (RCCs) and esters are widely occurred in plants and bacteria and are known to possess important bioactivities as mentioned earlier [37]. In this context, for many years, our work was focused on synthesis and biological activities of CFA esters and more recently DFT based thermodynamic calculations of CFA esters [12]. In this paper, preparation of several 2,3-*O*-protected 4-*O*-acyl rhamnopyranoside esters with *in vitro* antimicrobial activity tests is reported. The findings were further explained with DFT related studies.

2. Results and Discussion

2.1. Synthesis of benzyl 2,3-*O*-isopropylidene-α-L-rhamnopyranoside (4)

Initially, benzyl α-L-rhamnopyranoside (**3**) was prepared from L-rhamnose and benzyl alcohol in 82% yield (Scheme 1) as a chromatographically homogeneous brownish syrup which resisted crystallization [38].

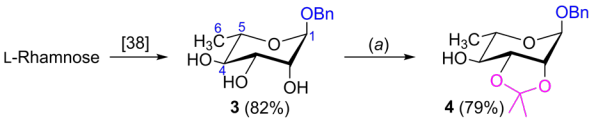

Scheme 1. Reagents and conditions: (*a*) DMP (excess), *p*-TSA (cat.), reflux, 30 min.

Having benzyl α-L-rhamnopyranoside (**3**) in hand, we have protected its *cis*-vicinal glycol group at C-2 and C-3 positions by isopropylidene protecting group. Thus, reaction of benzyl α-L-rhamnopyranoside (**3**) with 2,2-dimethoxypropane (DMP) in the presence of catalytic amount of *para*-toluenesulfonic acid (*p*-TSA) under reflux afforded a thick liquid compound in 79% yield (Scheme 1). Due to their *cis*-vicinal relationship, the probability of isopropylidene ring formation in the aforementioned reaction is in between C-2 OH and C-3 OH groups. The formation of isopropylidene was evident from its FT-IR spectrum which exhibited a band at 1381 cm^{-1} due to the presence of an isopropylidene functionality [$C(CH_3)_2$] in the molecule. Also a broad band at 3300-3450 cm^{-1} was due to hydroxyl group stretching. Further evidence in favour of the formation of monoacetonide comes from the analysis of its ^1H NMR spectrum. It displayed two three-proton singlets at δ 1.33 and 1.32 corresponding to two methyl groups of one isopropylidene ring. Also, one proton broad singlet at δ 1.90-2.20, which exchanged with D_2O, indicated the presence of only one hydroxyl group in the molecule. The rest of the protons were found reasonable with that of its precursor compound **3**. Hence, on the basis of complete analyses of

FT-IR and ^{1}H NMR spectra, the structure of the compound was established as benzyl 2,3-*O*-isopropylidene-α-L-rhamnopyranoside (**4**). Also, the spectral data of this **4** are in agreement with the previously isolated similar compound's data [39].

2.2. Synthesis of benzyl 4-*O*-acyl-2,3-*O*-isopropylidene-α-L-rhamnopyranosides 5-8

In the benzyl 2,3-*O*-isopropylidene-α-L-rhamnopyranoside (**4**) C-4 OH remains free. We have used this position for the synthesis of 4-*O*-acyl esters employing four different acylating agents. The synthesis was carried out by using direct acylation technique [33].

Our first attempt was to prepare 4-*O*-acetate of benzyl 2,3-*O*-isopropylidene-α-L-rhamnopyranoside (**4**). Therefore, a mixture of **4** and acetic anhydride in pyridine was stirred at room temperature for overnight. This upon usual work-up and purification afforded a white solid, mp 88-89 °C in 93% yield (Scheme 2).

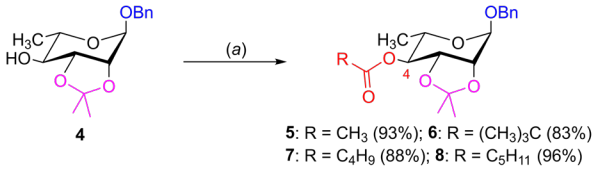

Scheme 2. Reagents and conditions: (*a*) Ac_2O/$(CH_3)_3CCOCl$/C_4H_9COCl/$C_5H_{11}COCl$ (1.1 eq.), pyridine (1 mL), DMAP (cat.), 0 °C-rt, 12-14 h.

In the FT-IR spectrum of this solid, a carbonyl stretching peaks was observed at 1733 cm^{-1} and a band at 1378 cm^{-1} was due to isopropylidene functionality. But, absence of frequency corresponding to OH group(s) indicated the acetylation of the molecule. In its ^{1}H NMR spectrum, a three-proton doublet at δ 1.24 (*J* = 6.2 Hz) was assigned for C-6 methyl protons. In the spectrum, a three-proton singlet at δ 2.18 was indicative of the attachment of acetyl group in the molecule ($COCH_3$). The H-4 proton appeared downfield at δ 4.84 (as dd, *J* = 9.8 and 6.6 Hz) as compared to δ 4.42-4.48 (as m, H-4) of its precursor monoacetonide, **4**. This downfield shift of H-4 proton was indicative of the attachment of acetyloxy groups at C-4 position. The molecular formula $C_{24}H_{26}O_8$ of the compound was in good agreement with the analytical data. Based on the above FT-IR and ^{1}H NMR data, the structure of the compound was unambiguously assigned as benzyl 4-*O*-acetyl-2,3-*O*-isopropylidene-α-L-rhamnopyranoside (**5**).

In the subsequent step reaction of monoacetonide **4** with bulky acylating agent like trimethylacetyl or pivaloyl chloride (PivCl) for overnight gave a faster moving single product. Usual work-up and chromatographic purification gave a semi-solid in 83% yield (Scheme 2). In its FT-IR spectrum, signals at 1740 and 1375 cm^{-1} were due to the carbonyl and isopropylidene groups, respectively. It showed no peaks corresponding to hydroxyl stretching and hence indicated the pivaloylation of the molecule. In the ^{1}H NMR spectrum, a five-proton multiplet at δ 7.29-7.40 was due to aromatic protons. Four characteristics singlets at δ 2.09 (3H, CH_3), 1.57 (6H, 2×CH_3), 1.56 (3H, CH_3) and 1.34 (3H, CH_3) were observed for fifteen protons. Of these six protons were due to two methyl groups for one isopropylidene functionality. The rest nine protons were assigned for one trimethylacety (pivaloyl) group attached to the molecule. A three-proton doublet (*J* = 6.4 Hz) at δ 1.16 was due to C-6 methyl protons. More importantly, considerable down field shift of H-4 at δ 4.88 (as dd, *J* = 10.0 and 6.8 Hz) than that of its precursor monoacetonide **4** (H-4 resonated at δ 4.42-4.48 as multiplet) indicated the attachment pentanoyloxy group at C-4 position (Figure 2). These observations and complete analysis of the rest of the FT-IR and ^{1}H NMR spectra were in complete agreement with the structure accorded as benzyl 4-*O*-pivaloyl-2,3-*O*-isopropylidene-α-L-rhamnopyranoside (**6**).

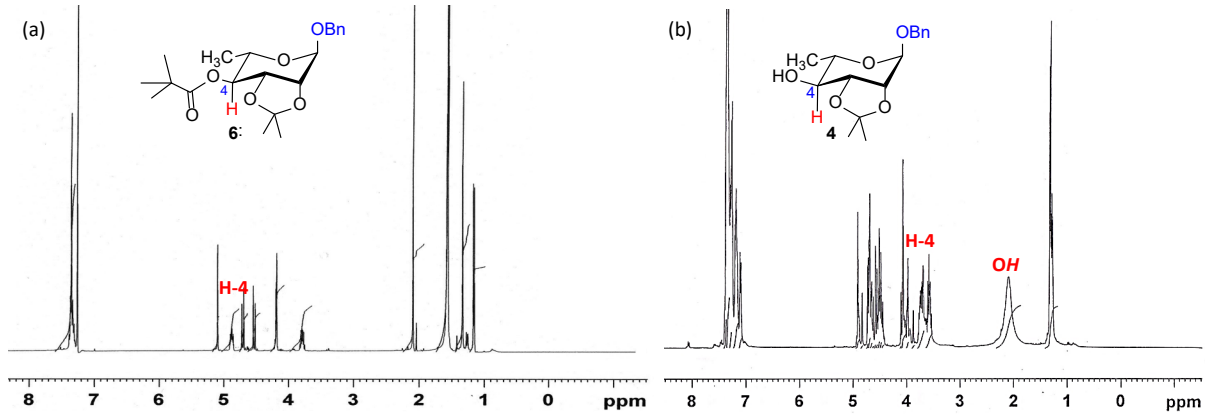

Fig. 2. Considerable downfield shift of H-4 proton in (a) **6** as compared to (b) **4**.

Similarly, pentanoylation of benzyl 2,3-*O*-isopropylidene-α-L-rhamnopyranoside (**4**) with little excess of pentanoyl chloride (PentCl) in anhydrous pyridine in the presence of DMAP (cat.) for 14 h afforded faster moving single product which upon chromatographic purification gave a clear oil (88%, Scheme 2). In its FT-IR spectrum, signals at 1734 and 1375 cm^{-1} were due to the carbonyl and isopropylidene groups, respectively. It also showed no peaks corresponding to hydroxyl stretching and hence indicated the pentanoylation of the molecule. In the ^{1}H NMR spectrum, a five-proton multiplet at δ 7.31-7.44 was due to aromatic protons. In the spectrum, a two-proton triplet at δ 2.33 (*J* = 7.5 Hz), a two-proton multiplet at δ 1.60-1.65, a two-proton multiplet at δ 1.21-1.27 and a three-proton triplet at δ 0.89 (*J* = 6.6 Hz) totaling nine protons were observed. Appearance of these extra protons as compared to its precursor compound **4** confirmed the incorporation of a penatanoyloxy group in the molecule. Considerable down field shift of H-4 at δ 4.88 than that of its precursor monoacetonide **4** indicated the attachment pentanoyloxy group at C-4 position. These

observations and complete analysis of the rest of the FT-IR and ^{1}H NMR spectra were in complete agreement with the structure accorded as benzyl 4-*O*-pentanoyl-2,3-*O*-isopropylidene-α-L-rhamnopyranoside (**7**).

Having success in these steps, we used hexanoyl chloride (HexCl) for acylation and obtained an oil in 92% yield (Scheme 2). The FT-IR spectrum of this oil exhibited no band for hydroxyl stretching. It also showed bands at 1734 and 1375 cm^{-1} corresponding to carbonyl and isopropylidene frequency, respectively and thus indicated the attachment of hexanoyl group in the compound. In its ^{1}H NMR spectrum, a two-proton triplet at δ 2.34, a two-proton multiplet at δ 1.61-1.66, a four-proton multiplet at δ 1.23-1.29 and a three-proton triplet at δ 0.87 for eleven protons corresponding to a hexanoyl group was observed. In the spectrum, a three-proton doublet at δ 1.18 was assigned for C-6 methyl protons. Two singlets at δ 1.58 and 1.31 were due to isopropylidene methyl protons. Considerable down field shift of H-4 at δ 4.89 as compared to that of its precursor monoacetonide **4** indicated the attachment hexanoyl group at C-4 position. Complete analysis of the rest of the FT-IR and ^{1}H NMR spectra led us to assign the structure as benzyl 4-*O*-hexanoyl-2,3-*O*-isopropylidene-α-L-rhamnopyranoside (**8**).

2.3. Antimicrobial activities

In vitro antibacterial activities were determined against four Gram-positive and four Gram-negative bacteria [40]. These are- *Bacillus cereus* BTCC 19, *Bacillus megaterium* BTCC 18, *Bacillus subtilis* BTCC 17, *Staphylococcus aureus* ATCC 6538, *Escherichia coli* ATCC 25922, *Klebsiella pneumonia* ATCC BAA 1705, *Pseudomonas aeruginosa* CRL (ICDDR, B), and *Salmonella typhi* AE 14612. The results are presented in Table 1. Isopropylidene protected rhamnopyranosides **4**-**8** showed weak potentiality against both the Gram-positive and Gram-negative organisms. 4-*O*-acetate **4** showed no zone of inhibition against *B. megaterium* (Figure 3a) while 4-*O*-hexanoate **8** showed little inhibition (10.9 mm, Figure 3b) against the same organism. Although incorporation of acyl groups increased some activity against Gram-positive bacteria than the Gram-negative pathogens, overall, the activities are weaker than the standard antibiotic ampicillin.

Table 1. Antibacterial effects of rhamnopyranoside **3**–**8**.

Organism	Diameter of zone of inhibition in mm (50 µg.dw / disc)						
	3	**4**	**5**	**6**	**7**	**8**	**APC**
				Gram-positive			
B. cereus	NI	8.5±.28	6.0±.50	NI	NI	NI	*22.0±.50
B. megaterium	NI	NI	5.5±.32	8.8±.33	6.5±.44	10.9±.68	19.5±.50
B. subtilis	NI	NI	NI	6.5±.50	5.5±.50	NI	*25.2±.34
S, aureus	NI	NI	NI	NI	NI	6.5±.50	*21.0±.50
				Gram-negative			
E. coli	NI	NI	NI	NI	NI	6.5±.50	*25.3±.68
K. pneumonia	NI	6.2±.33	NI	NI	NI	NI	*22.0±.50
P. aeruginosa	NI	NI	NI	NI	8.3±.48	NI	17.8±.28
S. typhi	NI	NI	NI	NI	NI	8.0±.50	13.2±.34

APC = ampicillin; NI = no inhibition; dw = dry weight; * = good inhibition

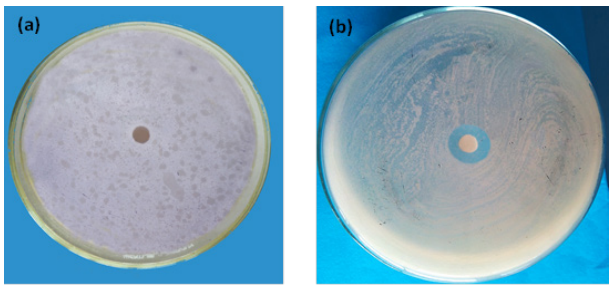

Fig. 3. Diameter of zone of inhibitions produced against *Bacillus megaterium* by (a) compound **4** and (b) compound **8**.

In vitro antifungal activities were assessed against two fungi namely *Aspergillus niger* ATCC 16404 and *Candida albicans* ATCC 10231 using literature procedure [41]. As shown in Table 2 protected rhamnopyranosides showed moderate antifungal potentiality against the tested organisms. These compounds are more prone against *C. albicans* than the *A. niger*. 4-*O*-acetate **4** showed 58.8% (Figure 4a) and 4-*O*-pentanoate **7** showed 50% (Figure 4b) inhibition zone against *C. albicans* although lower than the standard fungal drug nystatin (*63.1%).

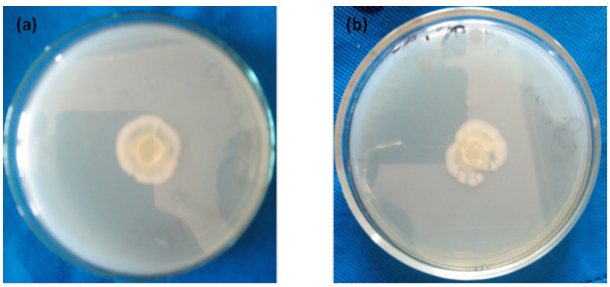

Fig. 4. Zone of inhibitions (%) produced against *Candida albicans* by (a) compound **4** and (b) compound **7**.

Table 2. *In vitro* antifungal effects of rhamnopyranoside **3**–**8**.

Organism	Percentage of zone of inhibition (50 µg.dw / ml PDA)						
	3	**4**	**5**	**6**	**7**	**8**	**NST**
A. niger	35.3±.59	30.5±.50	22.5±.50	29.0±.67	26.0±.50	32.0±.50	*66.4±.94
C. albicans	60.0±.84	58.8±.92	15.0±.33	38.8±.28	50.0±.79	48.9±.64	*63.1±.54

NST = nystatin; NI = no inhibition; dw = dry weight; * = good inhibition; PDA = potato dextrose agar

2.4. DFT based studies

2.4.1. Conformational analysis

The conformational behaviours of bioactive compounds are the basic factor for interactions with receptor proteins, and thus, all the compounds were optimized with Gaussian 09 program at B3LYP/6-31G basis set of DFT [42-43] at 298 K and 1 atm. It was observed that without isopropylidene ring fusion methyl α-L-rhamnopyranoside [44] and benzyl α-L-rhamnopyranoside (**3**) exist in the regular $^1C_4$ conformation (Figure 5). However, in the present case, 2,3-*O*-isopropylidene protection as in **4**-**8** and the presence of acyl group (acetyl, pivaloyl, pentanoyl, and hexanoyl) at C-4 position, increases the bulk in the molecule in addition to the presence glycosidic benzyl group. Therefore, it was thought to derive the conformations of rhamnopyranosides, **4**-**8** using DFT optimization and correlate with spectral data. The optimized conformational structures (tube model) at 298.15 K (1.0 atm) are shown in Figure 5 which were found to show C1 symmetry.

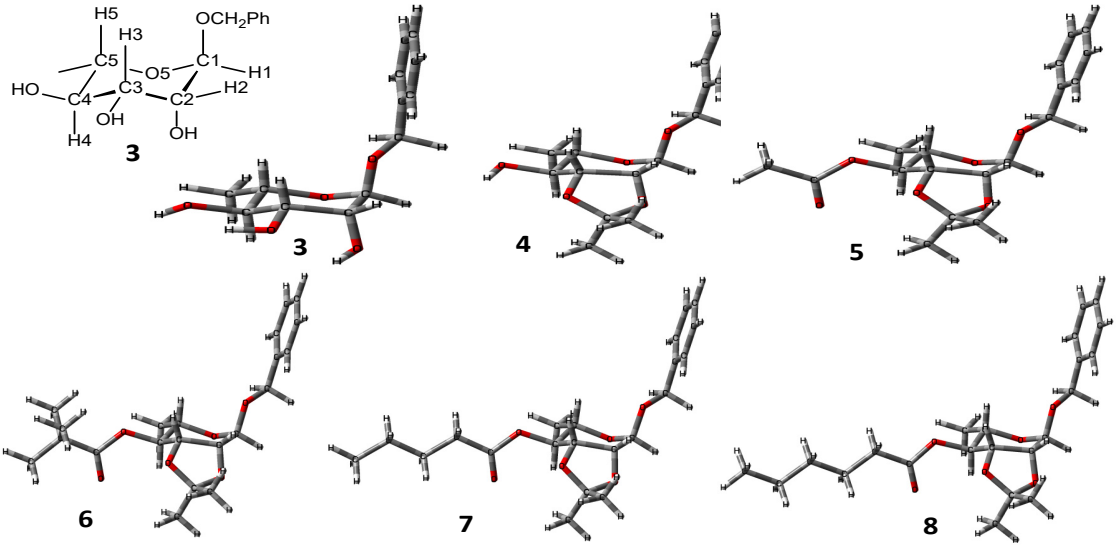

Fig. 5. DFT optimized structures of **3** and isopropylidene protected rhamnopyranoside **4**-**8**.

For conformational study of these benzyl rhamnopyranosides selected bond angles and dihedral angles as obtained from their optimized structures are mentioned in Table 3. It is clearly evident from the Table 3 that rhamnopyranoside **3** exist in regular $^1C_4$ conformation, while incorporation of 2,3-*O*-isopropylidene in the rhamnopyranoside skeleton increased bond angles at ∠O5-C1-C2, ∠C1-C2-C3 and ∠C2-C3-C4; and decreased at ∠C4-C5-O5 and ∠C5-O5-C1 positions than the compound **3**. We observed huge dihedral angle deviation due to the addition of five-membered isopropylidene ring in **4**-**8**. For example, dihedral angle at ∠H1-C1-C2-H2 increased (~7°) while highly decreased at ∠H2-C2-C3-H3 (~17°) and ∠H3-C3-C4-H4 (~14°) as compared to non-protected compound **3**. This huge deviation of dihedral angle imposed changed in their conformation and appeared as distorted $^1C_4$ conformation (Figure 5). We believe that the lower antimicrobial activities of **4**-**8** might be due to their conformational distortion.

Table 3. Bond angle and dihedral angle of rhamnopyranoside **3**-**8**.

Compound	Bond angle in degree					
	O5-C1-C2	**C1-C2-C3**	**C2-C3-C4**	**C3-C4-C5**	**C4-C5-O5**	**C5-O5-C1**
3	113.7	113.3	110.8	110.4	107.3	115.3
4	114.3	115.6	113.6	110.8	106.0	115.1
5	114.0	116.0	112.0	111.4	105.7	114.8
6	114.0	116.0	112.1	111.5	105.8	114.9
7	114.0	116.0	112.0	111.3	105.7	114.8
8	114.0	116.1	112.0	111.2	105.6	114.9
	Dihedral angle, in degree					
	H1-C1-C2-H2	H2-C2-C3-H3	H3-C3-C4-H4	H4-C4-C5-H5		
3	76.12	49.26	-177.54	-177.44		
4	83.93	32.40	-163.87	-174.68		
5	82.11	35.00	-162.59	-176.92		
6	82.26	34.79	-162.14	-177.45		
7	82.21	35.01	-162.71	-176.77		
8	82.82	34.94	-163.32	-176.24		

*All these values were calculated from 6-31G (B3LYP) sets

2.4.2. Thermodynamic analysis

As discussed earlier, fusion of 2,3-*O*-isopropylidene group in rhamnopyranoside ring imposed conformational distortion. Hence, we were interested to check the influence of such protecting group and ester group(s) towards thermodynamic properties of **4**-**8**. Several thermodynamic properties as obtained from the DFT optimized structures of **3**-**8** are summarized in Table 4.

Table 4. Molecular formula (MF), molecular weight (MW, g/mol), electronic energy (EE), enthalpy, Gibbs free energy (GFE), and dipole moment (DM) of **3**-**8**.

Compound No.	MF	MW	EE (Hartree)	Enthalpy (Hartree)	GFE (Hartree)	DM (Debye)
3	$C_{13}H_{18}O_5$	254.282	-882.0556	-881.7352	-881.7998	2.7199
4	$C_{16}H_{22}O_5$	294.350	-998.7613	-998.3750	-998.4466	1.3104
5	$C_{18}H_{24}O_6$	336.384	-1151.3750	-1150.9470	-1151.0282	2.5949
6	$C_{21}H_{30}O_6$	378.465	-1269.2887	-1268.7713	-1268.8606	2.5439
7	$C_{21}H_{30}O_6$	378.465	-1269.2885	-1268.7702	-1268.8612	2.3840
8	$C_{22}H_{32}O_6$	392.220	-1308.5925	-1308.0442	-1308.1387	2.3511

* EE indicates RB3LYP energy

With the increase of MW the negative value of EE, enthalpy and GFE gradually increased as usual. However, addition of acetonide group decreased dipole moment (μ) (as in **4**, ~1.3 Debye) than the non-protected **3** (~2.72 Debye). Also, incorporation of different acyl group(s) at C-4 position (as in **5**-**8**) slightly increased μ than **4**, but lower than the non-protected non-ester **3** (Table 4). It is well-known that μ is the measure of net molecular polarity, and improved μ can enhance hydrogen bond, and non-bonded interactions in drug receptor complexes which can play an important role to increase binding affinity [34]. The decreased and lower value of μ as in as in monoacetonide protected **4**-**8** (1.3-2.6 Debye, Table 4) clearly indicated their lower polar nature and lower binding affinity with target enzyme during antimicrobial activities. This may be the one of reasons for lower antimicrobial efficacy of these protected rhamnopyranosides **4**-**8**.

2.4.3. Molecular orbitals (MO) analysis

The HOMO (highest occupied molecular orbital), LUMO (lowest unoccupied molecular orbital) energy levels, HOMO-LUMO gap, hardness and softness of **3**-**8** are shown in Table 5. The HOMO-LUMO gaps between different molecules speak volumes about organic reactivity. These gaps within molecules help us understand the colours they emit/reflect. Also, FMO (frontier molecular orbital theory) indicated that HOMO-LUMO gaps have influence on the consequences in organic reactivity of the molecule.

Table 5. Energy (eV) of HOMO, LUMO, energy gap, hardness, and softness of **3**-**8**.

Drug	εHOMO	εLUMO	Gap	Hardness (*η*)	Softness (*S*)
3	-6.608	-0.0376	6.570	3.285	0.304
4	-6.660	-0.120	6.540	3.270	0.306
5	-6.730	-0.191	6.539	3.270	0.306
6	-6.728	-0.197	6.531	3.266	0.306
7	-6.722	-0.184	6.538	3.269	0.306
8	-6.726	-0.196	6.530	3.265	0.306

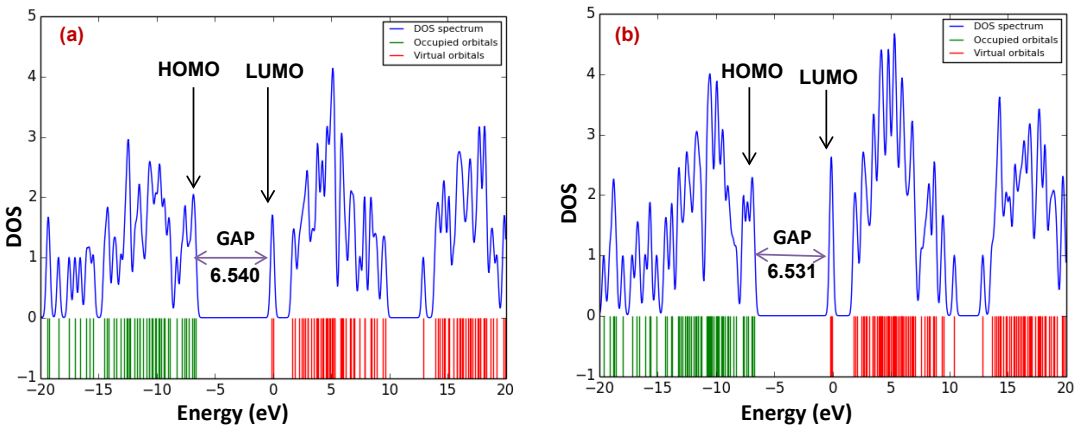

Figure 6. DOS plot and HOMO-LUMO energy gap of compound (a) **4**, and (b) **6**.

It is clear from the Table 5 that rhamnopyranoside **3** and isopropylidene protected rhamnopyranoside **4** possess almost similar HOMO-LUMO gap. Even attachment of the ester group at C-4 position, as in **5**-**8**, didn't change the gap. Previously, it was observed that with the attachment of acyl (ester) group(s) in sugar molecule HOMO-LUMO gap substantially decreased than the non-ester sugar compounds [34]. In the present case, the presence of a five-membered isopropylidene ring ar C-2 and C-3 positions of the six-membered rhamnopyranoside ring exerted distortion in the sugar ring and ultimately affect HOMO-LUMO Gap. Thus, all the rhamnopyranoside **3**-**8** showed almost similar hardness and softness values. That means even though the addition of acyl group(s) compound **4**-**8** had similar stability and reactivity.

3. Material and Methods

3.1. Materials and instrumentation

For synthetic purposes analytical grade reagents were purchased (Aldrich), and were used as received unless otherwise specified. Necessary pure solvents were used and purified if needed. Melting point was taken in an electro-thermal melting point apparatus and is uncorrected. Thin layer chromatography (TLC) was conducted on silica gel (Kieselgel GF_{254}) plates and the plate(s) was heated at 150–180 °C

spraying with methanolic H_2SO_4 (1%) untill blackish spot(s) appeared. For concentration all the mixtures were evaporated below 40 °C in a Buchi rotary evaporator (R-100, Switzerland) under reduced pressure. Purification of the compounds was carried out by the silica gel (G_{60}) column chromatography. The solvent system employed for the CC was *n*-hexane to *n*-hexane/ethyl acetate in different ratios. Characterization(s) of the synthesized compounds were accomplished by scanning and analyzing their FT-IR and ^{1}H NMR (400 MHz) spectra. ^{1}H NMR spectra were recorded in $CDCl_3$ solution in a tunable multinuclear probe (Bruker DPX-400 spectrometer, Switzerland). TMS was used as internal standard and chemical shifts were reported in δ unit (ppm). Coupling constant (*J*) values are shown in Hz. Elemental analyses were performed with a C,H-analyzer (EuroVector, EA3100).

3.2. Synthesis

Benzyl α-L-rhamnopyranoside (3): The title compound **3** was prepared from commercially available L-rhamnose, benzyl alcohol and Amberlite IR 120 (H^+) ion exchange resin in 82% yield as a colorless thick liquid using reported procedure [38].

Benzyl 2,3-O-isopropylidene-α-L-rhamnopyranoside (4): To a solution of benzyl α-L-rhamnopyranoside (**3**) (2.0 g, 7.865 mmol) and 2,2-dimethoxyprpane (DMP, 40 mL) was added catalytic amount of *para*-toluenesulfonic acid (*p*-TSA, 0.02 mg) at room temperature. Here DMP acts both as a solvent and as a reagent. The reaction mixture was refluxed for 30 min while TLC indicated the completion of the reaction. The mixture was allowed to attain room temperature, added 10% $NaHCO_3$ solution (2 mL) and extracted with ethyl acetate (3×5 mL). The organic layer was dried ($MgSO_4$) and concentrated in vacuum to leave a thick syrup which on column chromatography (*n*-hexane/ethyl acetate = 10/1) afforded the title compound **4** as an oil (1.829 g, 79%). R_f = 0.45 (*n*-hexane/ethyl acetate = 4/1); FT-IR ($CHCl_3$): 3300-3450 (br, OH), 1381 cm^{-1} [$C(CH_3)_2$]; ^{1}H NMR (400 MHz, $CDCl_3$): δ_H 7.09-7.36 (m, 5H, Ar-*H*), 4.92 (s, 1H, H-1), 4.72 (d, *J* =11.8 Hz, 1H, PhCH_AH$_B$), 4.70 (d, *J* = 5.0 Hz, 1H, H-2), 4.66 (dd [apparent t], *J* = 6.9 and 5.8 Hz, 1H, H-3), 4.58 (d, *J* =11.8 Hz, 1H, PhCH$_A$$H_B$), 4.51-4.57 (m, 1H, H-5), 4.42-4.48 (m, 1H, H-4), 1.90-2.20 (br s, exchange with D_2O, 1H, O*H*), 1.33 (s, 3H, CH_3), 1.32 (s, 3H, CH_3), 1.28 (d, *J* = 6.1 Hz, 3H, 6-CH_3); Anal. Calcd. for $C_{16}H_{22}O_5$ (294.35): C, 65.29; H, 7.53. Found: C, 65.32; H, 7.58.

3.2.1. General procedure for 4-O-acylation of rhamnopyranoside 4

Acylating agent(s) (1.1 molar eq, ~0.750 mmol) was added dropwise to a stirred solution of the monoacetonide (**4**) (0.2 g, 0.679 mmol) in anhydrous pyridine (1 mL) at 0 °C followed by addition of catalytic amount of DMAP [32]. The reaction mixture was stirred overnight at room temperature and TLC indicated the complete conversion of the starting compound into a faster moving product. The reaction mixture was treated with few drops of cold water to decompose excess acylating agent(s) and extracted with dichloromethane (3×3 mL). The organic layer was washed successively with 5% hydrochloric acid, saturated aqueous sodium hydrogen carbonate solution, brine and water. The organic layer was dried over $MgSO_4$ (anhydrous) and concentrated under diminished pressure. The residue thus obtained on silica gel column chromatography (*n*-hexane/ethyl acetate = 12/1) gave the corresponding 4-*O*-acyl esters **5**-**8** reasonably in high yields,

Benzyl 4-O-acetyl-2,3-O-isopropylidene-α-L-rhamnopyranoside (5): White solid, mp 88-89 °C; Yield 93% (0.212 g); R_f = 0.55 (*n*-hexane/ethyl acetate = 6/1); FT-IR ($CHCl_3$): 1733 (CO), 1378 cm^{-1} [$C(CH_3)_2$]; ^{1}H NMR (400 MHz, $CDCl_3$): δ_H 7.40-7.50 (m, 5H, Ar-*H*), 5.08 (s, 1H, H-1), 4.84 (dd, *J* = 9.8 and 6.6 Hz, 1H, H-4), 4.70 (d, *J* =11.8 Hz, 1H, PhCH_AH$_B$), 4.50 (d, *J* = 11.8 Hz, 1H, PhCH$_A$$H_B$), 4.19 (dd, *J* = 9.8 and 2.8 Hz, 1H, H-3), 4.17 (d, *J* = 2.8 Hz, 1H, H-2), 3.72-3.78 (m, 1H, H-5), 2.18 (s, 3H, COCH_3), 1.50 (s, 3H, CH_3), 1.31 (s, 3H, CH_3), 1.24 (d, *J* = 6.2 Hz, 3H, 6-CH_3); Anal. Calcd. for $C_{18}H_{24}O_6$ (336.38): C, 64.27; H, 7.19. Found: C, 64.34; H, 7.17.

Benzyl 2,3-O-isopropylidene-4-O-pivaloyl-α-L-rhamnopyranoside (6): Colorless semi-solid; Yield 83% (0.213 g); R_f = 0.59 (*n*-hexane/ethyl acetate = 6/1); FT-IR ($CHCl_3$): 1740 (CO), 1375 cm^{-1} [$C(CH_3)_2$]; ^{1}H NMR (400 MHz, $CDCl_3$): δ_H 7.29-7.40 (m, 5H, Ar-*H*), 5.10 (s, 1H, H-1), 4.88 (dd, *J* = 10.0 and 6.8 Hz, 1H, H-4), 4.71 (d, *J* =11.6 Hz, 1H, PhCH_AH$_B$), 4.53 (d, *J* = 11.6 Hz, 1H, PhCH$_A$$H_B$), 4.21 (dd, *J* = 9.8 and 2.8 Hz, 1H, H-3), 4.18 (1H, d, *J* = 2.8 Hz, H-2), 3.73-3.82 (1H, m, H-5), 2.09 (3H, s, CH_3), 1.57 (6H, s, 2×CH_3), 1.56 (s, 3H, CH_3), 1.34 (s, 3H, CH_3), 1.16 (d, *J* = 6.4 Hz, 3H, 6-CH_3); Anal. Calcd. for $C_{21}H_{30}O_6$ (378.47): C, 66.65; H, 7.99. Found: C, 66.70; H, 8.05.

Benzyl 2,3-O-isopropylidene-4-O-pentanoyl-α-L-rhamnopyranoside (7): Colorless oil; Yield 88% (0.226 g); R_f = 0.57 (*n*-hexane/ethyl acetate = 6/1); FT-IR ($CHCl_3$): 1734 (CO), 1375 cm^{-1} [$C(CH_3)_2$]; ^{1}H NMR (400 MHz, $CDCl_3$): δ_H 7.31-7.44 (m, 5H, Ar-*H*), 5.10 (s, 1H, H-1), 4.88 (dd, *J* = 9.7 and 6.5 Hz, 1H, H-4), 4.70 (d, *J* = 11.6 Hz, 1H, PhCH_AH$_B$), 4.55 (d, *J* = 11.6 Hz, 1H, PhCH$_A$$H_B$), 4.28 (dd, *J* = 9.7 and 2.8 Hz, 1H, H-3), 4.18 (d, *J* = 2.8 Hz, 1H, H-2), 3.75-3.80 (m, 1H, H-5), 2.33 [t, *J* = 7.5 Hz, 2H, $CH_3(CH_2)_2CH_2CO$], 1.60-1.65 (m, 2H, $CH_3CH_2CH_2CH_2CO$), 1.56 (s, 3H, CH_3), 1.33 (s, 3H, CH_3), 1.21-1.27 [m, 2H, $CH_3CH_2(CH_2)_2CO$], 1.16 (d, *J* = 5.8 Hz, 3H, 6-CH_3), 0.89 [t, *J* = 6.6 Hz, 3H, C$H_3(CH_2)_3CO$]; Anal. Calcd. for $C_{21}H_{30}O_6$ (378.47): C, 66.65; H, 7.99. Found: C, 66.64; H, 7.96.

Benzyl 2,3-O-isopropylidene-4-O-hexanoyl-α-L-rhamnopyranoside (8): Colorless syrup; Yield 96% (0.256 g); R_f = 0.59 (*n*-hexane/ethyl acetate = 6/1); FT-IR ($CHCl_3$): 1734 (CO), 1375 cm^{-1} [$C(CH_3)_2$]; ^{1}H NMR (400 MHz, $CDCl_3$): δ_H 7.52-7.66 (m, 5H, Ar-*H*), 5.08 (s, 1H, H-1), 4.89 (dd, *J* = 9.9 and 6.6 Hz, 1H, H-4), 4.72 (d, *J* = 11.6 Hz, 1H, PhCH_AH$_B$), 4.54 (d, *J* = 11.6 Hz, 1H, PhCH$_A$$H_B$), 4.26 (dd, *J* = 9.9 and 2.9 Hz, 1H, H-3), 4.19 (d, *J* = 2.9 Hz, 1H, H-2), 3.71-3.77 (m, 1H, H-5), 2.34 [t, *J* = 7.4 Hz, 2H, $CH_3(CH_2)_3CH_2CO$], 1.61-1.66 [m, 2H, $CH_3(CH_2)_2CH_2CH_2CO$], 1.58 (s, 3H, CH_3), 1.31 (s, 3H, CH_3), 1.23-1.29 [m, 4H, $CH_3(CH_2)_2(CH_2)_2CO$], 1.18 (d, *J* = 6.0 Hz, 3H, 6-CH_3), 0.87 [t, *J* = 6.5 Hz, 3H, C$H_3(CH_2)_4CO$]; Anal. Calcd. for $C_{22}H_{32}O_6$ (392.49): C, 67.32; H, 8.22. Found: C, 67.36; H, 8.28.

3.3. *In vitro* antimicrobial tests

Screening of antibacterial activity: For the detection of antibacterial activity, the disc diffusion method [40] was used against four Gram-positive and four Gram-negative bacteria. Dimethylformamide (DMF) was used as a solvent for the test chemicals, and a 2% solution of each compound was used. The plates were incubated at 37 °C for 48 h. Proper control was maintained with DMF without chemicals. Mueller-Hinton (agar and broth) medium was used to culture the bacteria. All of the results were compared to the standard antibacterial antibiotic ampicillin (50 µg/disc, brand name Decapen, Beximco Pharmaceuticals Ltd., Bangladesh). Each experiment was carried out three times.

Screening of mycelial growth: The antifungal activities of the rhamnopyranosides **3**-**8** were determined according to food poisoning technique [41] against two fungi. Sabouraud (agar and broth, PDA) medium was used for culture of fungi. Linear mycelial growth of fungus was measured after 3~5 days of incubation. The percentage inhibition of the radial mycelial

growth of the test fungus was calculated as: I = [(C-T)/C]×100. Where, I = percentage of inhibition, C = diameter of the fungal colony in the control (DMF) and T = diameter of the fungal colony in the treatment. The results were compared with the standard antifungal antibiotic nystatin (50 µg/mL PDA, brand name Fungistin, Beximco Pharmaceuticals Ltd., Bangladesh).

3.3. Computational calculations

In the last few decades DFT (density function theory) based quantum mechanical methods are used to predict thermal energies, molecular orbital (MO), and molecular electrostatic potential (MEP) properties [43]. In the present study, the basic geometry of the benzyl α-L-rhamnopyranoside (**3**) was taken from the online structure database namely ChemSpider. The other structures of **4**-**8** were drawn in the *GaussView* (5.0) program [42] keeping the appropriate stereochemistry of the molecules. These molecules were then optimized with Gaussian 09 program at B3LYP/6-31G basis set of DFT [42, 45] at 298 K and 1 atm. We have used GaussSum 3.0 to get DOS plot. FMO (frontier molecular orbital) energy like HOMO (highest occupied molecular orbital), LUMO (lowest unoccupied molecular orbital), HOMO-LUMO gap, hardness (η), and softness (S) were calculated at the same level of DFT theory using the following equations:

$$\text{Gap} = [\varepsilon\text{LUMO} - \varepsilon\text{HOMO}]; = \frac{\varepsilon LUMO - \varepsilon HOMO}{2}; S = \frac{1}{\eta}$$

4. Conclusions

Thus, 4-*O*-acyl-2,3-*O*-isopropylidene-α-L-rhamnopyranosides **5**-**8** were successfully prepared from benzyl α-L-rhamnopyranoside (**3**). These synthesized compounds were characterized by spectroscopic techniques. *In vitro* antimicrobial activity test against eight bacterial and two fungal pathogens indicated that these compounds had weak antimicrobial efficacy. DFT based conformational study along with thermodynamic and FMO theory signified that the lower antimicrobial efficacy was due to conformational distortion, higher hardness, lower softness and smaller dipole moments of these monoacetonide protected rhamnopyranoside esters.

Acknowledgments

Partial financial support from the Research and Publication Cell, University of Chittagong, Bangladesh (2021, Special) is highly acknowledged.

Author Contributions

MM Matin, D Muhammad and SMR Miah designed and synthesized the compounds. P Devi designed and completed computational study. All authors are involved in the interpretation and validation of spectral data, writing and approved the final version of the work. MM Matin managed the project fund.

References and Notes

1] Fan, P.; Terrier, L.; Hay, A. E.; Marston, A.; Hostettmann, K. *Fitoterapia* **2010**, *81*, 124. [Crossref]

[2] Liu, P.; Hu, Y.; Guo, D. H.; Wang, D. X.; Tu, H. H.; Ma, L.; Xie, T. T.; Kong, L. Y. *Phytomedicine* **2010**, *17*, 794. [Crossref]

[3] Chang, C. L.; Zhang, L. J.; Chen, R. Y.; Kuo, L. M. Y.; Huang, J. P.; Huang, H. C.; Lee, K. H.; Wu, Y. C.; Kuo, Y. H. *J. Nat. Prod.* **2010**, *73*, 1482. [Crossref]

[4] Takasaki, M.; Konoshima, T.; Kuroki, S.; Tokuda, H.; Nishino, H. *Cancer Lett.* **2001**, *173*, 133. [Crossref]

[5] Matin, M. M.; Bhuiyan, M. M. H.; Kabir, E.; Sanaullah, A. F. M.; Rahman, M. A.; Hossain, M. E.; Uzzaman, M. *J. Mol. Struct.* **2019**, *1195*, 189. [Crossref]

[6] Chansanroj, K.; Betz, G. *Acta Biomaterialia* **2010**, *6*, 3101. [Crossref]

[7] Huang, X. B.; Zhang, B. C.; Xu, H. *Bioorg. Med. Chem. Lett*. **2017**, *27*, 4336. [Crossref]

[8] Perinelli, D. R.; Lucarini, S.; Fagioli, L.; Campana, R.; Vllasaliu, D.; Durant,i A.; et al. *Eur. J. Pharm. Biopharm*. **2018**, *124*, 55. [Crossref]

[9] AlFindee, M. N.; Zhang, Q.; Subedi, Y. P.; Shrestha, J. P.; Kawasaki, Y.; Grilley, M.; et al. *Bioorg. Med. Chem*. **2018**, *26*, 765. [Crossref]

[10] Aronson, M.; Medalia, O.; Schori, L.; Mirelman, D.; Sharon, N.; Ofek, I. *J. Infect. Dis*. **1979**, *139*, 329. [Crossref]

[11] Matin, M. M. *Orbital: Electron. J. Chem*. **2014**, *6*, 20. [Crossref]

[12] Matin, M. M.; Uzzaman, M.; Chowdhury, S. A.; Bhuiyan, M. M. H. *J. Biomol. Struct. Dyn*. [Crossref]

[13] Valverde, P.; Ana Ardá, A.; Reichardt, N. C.; Jiménez-Barbero, J.; Gimeno, A. *Med. Chem. Commun.* **2019**, *10*, 1678. [Crossref]

[14] Linhardt, R. J. *J. Med. Chem*. **2003**, *46*, 2551. [Crossref]

[15] Herbert, J. M.; Petitou, M.; Lormeau, J. C.; Cariou, R.; Necciari, J.; Magnani, H. N.; Zandberg, P.; van Amsterdam, R. G. M.; van Boeckel C. A. A.; Meuleman, D. G. *Cardiovasc. Drug Rev.* **1997**, *15*, 1. [Crossref]

[16] Krasnova, L.; Chi-Huey Wong, C-. H. *J. Am. Chem. Soc.* **2019**, *141*, 3735. [Crossref]

[17] Kim, S. R.; Kim, Y. C. *Phytochem*. **2000**, *54*, 503. [Crossref]

[18] Dong, X. Z.; Huang, C. L.; Yu, B. Y.; Hu, Y.; Mu, L. H.; Liu, P. *Phytomedicine* **2014**, *21*, 1178. [Crossref]

[19] Tian, Y.; Liu, W.; Lu, Y.; Wang, Y.; Chen, X.; Bai, S.; Zhao, Y.; He, T.; Lao, F.; Shang, Y.; Guo, Y. She, G. *Molecules* **2016**, *21*, 1402. [Crossref]

[20] Mihoub, M.; Pichette, A.; Sylla, B.; Gauthier, C.; Legault, J. *PLoS ONE* **2018**, *13*, 0193386. [Crossref]

[21] McCranie, E. K.; Bachmann, B. O. *Nat. Prod. Rep.* **2014**, *31*, 1026. [Crossref]

[22] Islam, F.; Rahman, M. R.; Matin, M. M. *Turkish Comp. Theo. Chem.* **2021**, *5*, 39. [Crossref]

[23] Qian, J.; Hunkler, D.; Rimpler, H. *Phytochemistry* **1992**, *31*, 905. [Crossref]

[24] Duck, J. A.; Ayensu, E.; S. Medical Plants of China. Algonac, MI, 1985.

[25] Akong, F. O.; Bouquillon, S. *Green Chem*. **2015**, *17*, 3290. [Crossref]

[26] Yang, X. −D.; Li, Z. −Y.; Mei, S. −X.; Zhao, J. −F.; Zhang, H. −B.; Li, L. *J. Asian Nat. Prod. Res*. **2003**, *5*, 223. [Crossref]

[27] Lawandi, J.; Rocheleau, S.; Moitessier, N. *Tetrahedron* **2016**, *72*, 6283. [Crossref]

[28] Kiyoshima, K.; Sakamoto, M.; Ishikura, T.; Fukagawa, Y.; Yoshioka, T.; Naganawa, H.; Sawa, T.; Takeuchi, T. *Chem. Pharm. Bull.* **1989**, *37*, 861. [Crossref]

[29] Jäger, M.; Minnaard, A. *J. Chem. Commun.* **2016**, *52*, 656. [Crossref]

[30] Buzatu, A. R.; Frissen, A. E.; van den Broek, L. A. M.; Todea, A.; Motoc, M.; Boeriu, C. G. *Processes* **2020**, *8*, 1638. [Crossref]

[31] Richel, A.; Laurent, P.; Wathelet, B.; Wathelet, J. –P.; Paquot, M. *Comptes Rendus Chimie* **2011**, *14*, 224. [Crossref]

[32] Ren, B.; Zhang, L.; Zhang, M. *Asian J. Org. Chem*. **2019**, *8*, 1813. [Crossref]

[33] Matin, M. M. *J. Appl. Sci. Res*., **2008**, *4*, 1478. [Link]

[34] Matin, M. M.; Iqbal, M. Z. *Orbital: Electron. J. Chem*. **2021**, *13*, 19. [Crossref]

[35] Tsuda, Y.; Haque, M. E.; Yoshimoto, K. *Chem. Pharm. Bull.* **1983**, *31*, 1612. [Crossref]

[36] Ghoneim, A. A. *Chem. Central J*. **2011**, *5*, 7. [Crossref]

[37] Lu, L.; Liu, Q.; Jin, L.; Yin, Z.; Xu, L.; Xiao, M. *PLoS One* **2015**, *10,* e0140531. [Crossref]

[38] Brimacombe, J. S.; Cook, M. C.; Tucker, L. C. N. *J. Chem. Soc*. **1965**, 2292.

[39] Bedini, E.; Parrilli, M.; Unverzagt, C. *Tetrahedron Lett.* **2002**, *43*, 8879. [Crossref]

[40] Matin, M. M.; Hasan, M. S.; Uzzaman, M.; Bhuiyan, M. M. H.; Kibria, S. M.; Hossain, M. E.; Roshid, M. H. O. *J. Mol. Struct*. **2020**, *1222*, 128821. [Crossref]

[41] Grover, R. K.; Moore, J. D. *Phytopathol*. **1962**, *52*, 876.

[42] Frisch, M. J.; Trucks, G. W.; Schlegel, H. B.; Scuseria, G. E.; Robb, M. A.; Cheeseman, J. R.; Scalmani, G.; Barone, V.; Petersson, G. A.; Nakatsuji, H. Gaussian 09, **2013**, Gaussian, Inc. (Wallingford CT).

[43] Matin, M. M.; Chakraborty, P.; Alam, M. S.; Islam, M. M.; Hanee, U. *Carbohydr. Res*. **2020**, *496*, 108130. [Crossref]

[44] Shalaby, M. A.; Fronczek, F. R.; Younathan, E. S. *Carbohydr. Res*. **1994**, *258*, 267. [Crossref]

[45] Islam, M. T.; Kumer, A.; Chakma, U.; Howlader, D. *Orbital: Electron. J. Chem*. **2021**, *13*, 58. [Crossref]

How to cite this article

Muhammad, D.; Matin, M. M.; Miah, S. M. R.; Devi, P. *Orbital: Electron. J. Chem*. **2021**, *13*, 250. DOI: http://dx.doi.org/10.17807/orbital.v13i3.1614